Cancer Biology & Therapy

ISSN: 1538-4047 (Print) 1555-8576 (Online) Journal homepage: http://www.tandfonline.com/loi/kcbt20

Differential sensitivity of A549 non small lung carcinoma cell responses to epidermal growth factor receptor pathway inhibitors

Maria L. Jaramillo, Myriam Banville, Catherine Collins, Beatrice Paul-Roc, Lucie Bourget & Maureen O'Connor-McCourt

To cite this article: Maria L. Jaramillo, Myriam Banville, Catherine Collins, Beatrice Paul-Roc, Lucie Bourget & Maureen O'Connor-McCourt (2008) Differential sensitivity of A549 non small lung carcinoma cell responses to epidermal growth factor receptor pathway inhibitors, Cancer Biology & Therapy, 7:4, 557-568, DOI: 10.4161/cbt.7.4.5533

To link to this article: http://dx.doi.org/10.4161/cbt.7.4.5533

Published online: 01 May 2008.

[Cancer Biology & Therapy 7:4, 557-568; April 2008]; ©2008 Landes Bioscience

Research Paper

Differential sensitivity of A549 non-small cell lung carcinoma cell responses to epidermal growth factor receptor pathway inhibitors

Maria L. Jaramillo,[1,*] Myriam Banville,[1] Catherine Collins,[1] Beatrice Paul-Roc,[1] Lucie Bourget[1] and Maureen O'Connor-McCourt,[1,2]

[1]Biotechnology Research Institute; National Research Council of Canada; Montreal, Quebec Canada; [2]Department of Biochemistry; McGill University; Montreal, Quebec Canada

Abbreviations: NSCLC; non-small cell lung cancer, EGF; epidermal growth factor, EGFR; epidermal growth factor receptor, mAb; monoclonal antibody, TKI; tyrosine kinase inhibitor, EMT; epithelial-mesenchymal transition, PBS; phosphate buffered saline, FBS; fetal bovine serum

Key words: epidermal growth factor receptor, AG1478, 225 mAb, anchorage-independent growth, motility, antibody, tyrosine kinase inhbitor

It has been demonstrated that A549 non-small cell lung cancer (NSCLC) cells are sensitive to epidermal growth factor receptor (EGFR) inhibitors in in vivo xenograft animal models, but are relatively resistant in conventional in vitro monolayer growth assays. Here, we utilized anchorage-independent cell growth/survival assays as well as motility assays and demonstrated that these tests detect the effects of two EGFR inhibitors, the small molecule inhibitor AG1478 and the ligand-blocking antibody 225 mAb, on A549 cells more sensitively than monolayer growth assays. AG1478 was more effective than 225 mAb at inhibiting EGF-stimulated anchorage-independent cell growth, in part due to its pronounced ability to inhibit cell survival, whereas 225 mAb and AG1478 were both able to inhibit cell motility. In order to determine which EGFR signalling pathway components were most strongly associated with these cell responses, we analyzed in parallel the phosphorylation levels of EGFR itself as well as several downstream pathway elements. We found that the limited ability of 225 mAb to inhibit MAPK, PI3K and STAT3 phosphorylation correlated with its inability to promote anchorage independent apoptosis, but did not correlate with its ability to inhibit motility. Based on our results in A549 cells, we propose that EGF stimulates tumour progression of NSCLC largely through effects on anchorage-independent growth and survival, as well as motility.

Introduction

Lung cancer remains the most common type of cancer in men and women worldwide[1] and is the leading cause of cancer-related deaths (2006, American Cancer Society) largely as a result of its highly metastatic nature. Due to the generally poor clinical response to conventional lung cancer treatments, increasing efforts are being made to develop novel treatment strategies directed against molecular therapeutic targets. Overexpression of epidermal growth factor receptor (EGFR) occurs in 40–80%[2] of non-small cell lung cancers (NSCLC) and is correlated with disease progression and resistance to chemotherapy.[3] Moreover, in many tumor types including lung, co-expression of EGFR ligands is common[3] suggesting the presence of activating autocrine loops. The epidermal growth factor receptor (EGFR) pathway contributes to a number of processes important to cancer development and progression, including cell proliferation, apoptosis, angiogenesis and metastatic spread.[4]

One therapeutic strategy designed to target EGF receptors involves the development of small molecule tyrosine kinase inhibitors (TKIs) directed against the adenosine triphosphate (ATP) binding site of the tyrosine kinase domain. AG1478 is the prototype for this class of compounds[5] and is frequently used as a potent and specific EGFR inhibitor in in vitro and cell-based assays.[6] This approach has been further developed resulting in a newer generation of EGFR antagonists for clinical use, such as gefitinib/ZD1839/Iressa*, (Astra Zeneca, see ref. 7) or erlotinib/Tarceva* (OSI/Genentech, see ref. 8). An alternative approach to targeting EGFR consists of the development of anti-receptor antibodies that block ligand binding, thereby interfering with growth factor receptor mediated autocrine and/or paracrine signaling, reviewed in ref. 9. One such anti-EGFR antibody, the humanized 225 monoclonal antibody (225 mAb), cetuximab (Erbitux*, Imclone), has also been used therapeutically.[10,11]

The pleotropic effects of EGFR activation are mediated by the activation of multiple downstream signalling proteins, including the extracellular-related kinase (ERK)/MAP kinase, phosphatidyl-inositiol-3' (PI-3) kinase (PI3K) and STAT3. MAPK and PI3K-AKT signaling are involved in EGFR-dependent growth and survival.[12] In addition, these signal transduction molecules have been implicated in tumor associated motility and invasion.[13,14] STAT3 has also been implicated in processes related to tumor cell survival and motility.[15,16]

*Correspondence to: Maria L. Jaramillo; Biotechnology Research Institute; National Research Council of Canada; 6100 Royalmount Avenue; Montreal, Quebec H4P 2R2 Canada; Tel.: 514.496.6384; Fax: 514.496.5143; Email: maria.jaramillo@nrc.ca

Submitted: 10/16/07; Revised: 12/21/07; Accepted: 01/07/08

Previously published online as a *Cancer Biology & Therapy* E-publication: http://www.landesbioscience.com/journals/cbt/article/5533

In NSCLC in particular, EGFR-STAT3 signalling has been shown to promote tumor growth and survival in vitro and in vivo.[17]

The A549 cell line is a well-studied lung adenocarcinoma cell line that is characterized with respect to K-ras and p53 status, as well as other factors. A549 cells contain an activating K-ras mutation, which is commonly found in NSCLC tumors and corresponding cell lines.[18] As part of the NCI-60 tumor cell line panel, this cell line has been tested for its responsiveness to chemotherapeutics and various molecularly targeted therapeutics.[19] The A549 cell line has also been used in xenograft, including orthotopic, models of NSCLC to study primary tumor growth and metastasis.[20-24] Notably, A549 cells lack the EGFR kinase mutation that confers auto activation and EGFR TKI sensitivity and that has been detected in some sensitive lung cancer tumors and cell lines.[25-27]

Despite the fact that this cell line expresses high levels of surface EGFR[28] it has been previously characterized to exhibit low to intermediate[29-33] sensitivity to known EGFR inhibitors in conventional monolayer growth assays. More recently, however, it has been demonstrated that humanized 225 mAb (cetuximab) exhibits antitumor activity in xenograft models based on A549 cells as well as other NSCLC cell lines expressing EGFR.[34,35] In addition, other reports show that EGFR TKIs such as ZD1839 (gefitinib)[36,37] and erlotinib[38] exhibit anti-tumor activity in A549 xenograft tumors both as monotherapy, and in combination with chemotherapies or vascular targeting agents. The reason behind the discrepancy between the sensitivity of A549 cell growth to EGFR inhibitors in vitro versus in animal xenograft models is not clear. This differential sensitivity in vitro versus in vivo may relate in part to the effects of EGFR inhibitors on the tumor microenvironment, i.e., non-tumor cell actions, including known inhibitory effects on tumor vasculature.[39] However, the discrepancy may also result from the limited ability of conventional monolayer growth assays to accurately predict the direct effect of EGFR inhibitors on tumor cell behavior in vivo.

Although perhaps limited in predictive power, two-dimensional monolayer cell growth assays have traditionally been relied upon in preclinical studies designed to assess the efficacy of EGFR and other molecularly targeted inhibitors. These assays generally measure relatively short term growth of carcinoma cell lines usually through the evaluation of metabolic activity using reducing dyes such as MTT. These monolayer growth assays fail to measure anchorage-independent survival and growth, one of the distinguishing features of transformed cells.[40] On the other hand, assays performed under anchorage-independent conditions, such as colony-forming or clonogenic assays, tend to measure more accurately the in vivo tumorigenic potential of tumor cell lines.[41] An additional limitation of both monolayer and anchorage-independent tumor cell growth assays is their failure to take into account the effect of inhibitors on processes related to metastasis, such as motility and invasion. It has recently been proposed that increased cell motility and invasion may impact not only metastasis, but also growth at the primary tumor site. This "self-seeding" hypothesis postulates that cell motility may contribute to the high cell density, rapid growth rate and large primary tumor size of more aggressive tumors.[42] Accordingly, effects of inhibitors on primary tumor growth may also be underestimated if effects on motility and invasion are not assessed.

The goal of the current study was two-fold. First, we were interested in assessing the efficacy of EGFR inhibitors in quantitative anchorage-independent growth/survival and motility assays to determine if these tests could detect the effect of EGFR inhibitors on A549 phenotypic responses more sensitively than conventional monolayer growth assays. Our second objective was to correlate these A549 cellular responses with the phosphorylation of signalling pathway components in order to identify the pathway elements that were most strongly associated with different phenotypic behaviours. We utilized two EGFR inhibitors, the small molecule kinase inhibitor AG1478 and the ligand-blocking antibody 225 mAb, so that we could compare their potencies to affect both signaling pathway events and phenotypic responses. We observed that 225 mAb was less effective than AG1478 at inhibiting EGF-stimulated anchorage-independent growth, partly due to its inability to promote cell apoptosis. This correlated with 225 mAb's limited ability to inhibit MAPK, PI3K and STAT3 phosphorylation. 225 mAb and AG1478 both inhibited cell motility, in spite of their differential effects on downstream MAPK, PI3K and STAT3 phosphorylation. In summary, our results indicate that in vitro anchorage-independent growth/survival and motility assays are more appropriate measurements than monolayer growth assays for assessing EGFR inhibitor efficacy.

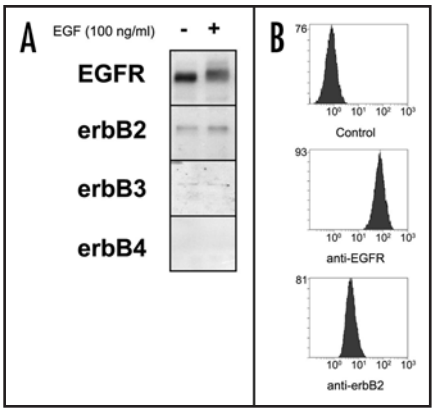

Figure 1. erbB expression in A549 cells. (A) A549 cell were treated in the absence or presence of EGF (100 ng/ml) for 10 minutes at 37°C prior to lysis. Cell lysates were subject to Western blotting with antibodies directed against various erbB family members. (B) Detection of cell surface EGFR and erbB2 on A549 cells by flow cytometry (as indicated in Materials and Methods).

Results

Expression of EGFR family members. As background for the study of the effect of EGF and EGFR inhibitors on A549 cell signaling pathways and phenotypic responses, we first determined the levels of expression of EGFR and related family members (erbB 2, 3, 4) in these cells (Fig. 1). Using Western blotting to assess the total levels of receptor (both intracellular and cell surface), we detected the presence of both EGFR and erbB2 (Fig. 1A). This is consistent with results from other studies on A549 cells[31,32] and is not unexpected considering that erbB2 and EGFR tend to be co-expressed in up to 80% of human lung adenocarcinoma tumor specimens[45] as well as in most cell lines derived from these tumors. We also observed a relatively low level of expression of erbB3, which is in agreement with a previous study in which mRNA transcripts encoding erbB3 were detected by RT-PCR in A549 cells.[46] We did not detect expression

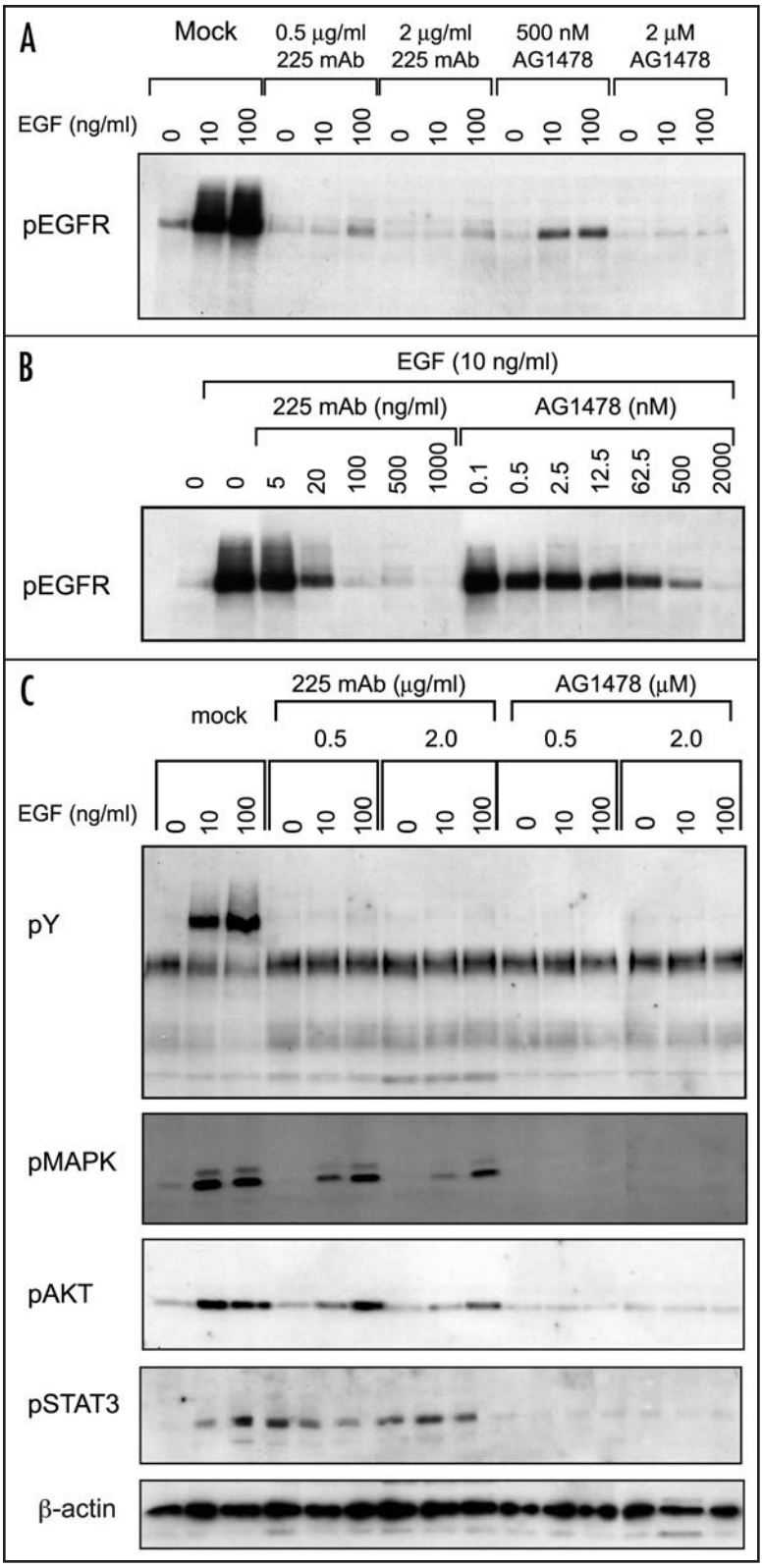

Figure 2. Effect of EGFR inhibitors on signal transduction pathways in A549 cells. A549 cells were pretreated with various concentrations of EGFR inhibitors, 225 mAb or AG1478, for 60 minutes prior to incubating for 10 minutes with EGF (as indicated). Cell lysates were subject to immunoblotting with phospho-specific EGFR (Y1068) (A and B), anti-phosphotyrosine, anti-phosphoMAPK, anti-phosphoAKT or phosphoSTAT3 antibodies (C). Protein loading was determined by blotting against β-actin (C).

of erbB4, which is also in agreement with the reported lack of erbB4 mRNA expression in this cell line.[46]

We next utilized flow cytometry analysis of live cells to examine the cell surface levels of EGFR and erbB2, i.e., the two EGFR family members that we detected as being expressed at significant amounts in these cells by Western blotting. Previously, using Scatchard analysis, we determined that approximately 150,000 EGFR molecules are expressed at the surface of A549 cells.[28] Here, we detected relatively high surface expression levels of EGFR (Fig. 1B), which is consistent with our Scatchard and Western blot results. By comparing the flow cytometry data for EGFR with that of erbB2 (Fig. 1B), we estimate that there are 12,000 surface erbB2 receptors per A549 cell (see Materials and Methods).

Effect of EGFR modulation on receptor phosphorylation and downstream signalling. Activated EGF receptors transduce extracellular signals to the cytoplasm by dimerizing with, and transphosphorylating, other erbB receptor molecules, and then phosphorylating downstream signalling proteins, reviewed in refs. 47 and 48. As the first step in our investigation of the effect of EGFR stimulation and inhibition on A549 signaling pathways, we assessed the ability of two concentrations of AG1478 (0.5 and 2.0 μM) and two concentrations of 225 mAb (0.5 and 2.0 μg/ml) to inhibit EGFR phosphorylation in the absence of added EGF, as well as following a 10 minute incubation in the presence of 10 or 100 ng/ml EGF. We monitored EGFR phosphorylation using either EGFR phosphorylation site-specific antibodies (Tyr1068—Fig. 2A and 2B Tyr845, 1086, 1173—data not shown) or an antibody detecting total phosphotyrosine (Fig. 2C). A basal level of EGFR phosphorylation was observed at all the sites with the level of phosphorylation being strongly induced by both 10 and 100 ng/ml EGF at all sites, as expected (Fig. 2A and data not shown). 225 mAb and AG1478 were observed to reduce the levels of both basal and EGF-stimulated EGFR phosphorylation at all sites in a dose dependent manner (Fig. 2A and B and data not shown). It is interesting to note that 225 mAb at 0.5 μg/ml (3.3 nM) and 2.0 μg/ml (13.2 nM) was able to inhibit EGF-stimulated phosphorylation more effectively at the lower concentration of EGF (10 ng/ml, 1.7 nM) as compared to the higher concentration of EGF (100 ng/ml, 17 nM) (Fig. 2A). This effect is likely due to the fact that EGF competes with 225 mAb for binding to the extracellular domain of EGFR.[49] In contrast, AG1478 was able to inhibit EGFR phosphorylation to the same extent at both EGF concentrations. This likely results from the fact that AG1478 targets the catalytic site rather than the ligand-binding site.

Next, using a range of AG1478 and 225 mAb concentrations, we determined the dose-response curve of each inhibitor for reducing EGF-stimulated EGFR phosphorylation. It can be seen that 1000 ng/ml 225 mAb and 2000 nM AG1478 effectively inhibited EGFR phosphorylation in the presence of 10 ng/ml of EGF (Fig. 2B). Accordingly, in subsequent experiments in which we examined downstream signaling and phenotypic responses, we used these inhibitors at concentrations in this range.

We next examined the effects of AG1478 and 225 mAb on phos-

phorylation of MAPK, AKT, and STAT3, three major components in pathways downstream of EGFR (as well as on tyrosine phosphorylation of EGFR/erbB as an internal control; Fig. 2C) following a 10 minute incubation with EGF. A low basal level of MAPK phosphorylation was observed using an antibody that detects phosphorylation on Thr183 and Tyr185 and, as expected, this was strongly induced by EGF. Similarly, a low basal level of activated AKT was observed, using an antibody that detects phosphorylation on Ser 473, which was further stimulated by EGF. Little basal activation of STAT3 (assessed by Tyr705 phosphorylation) was detected, however, as expected, EGF stimulated STAT3 phosphorylation. Consistent with our results obtained using EGFR phosphorylation site-specific antibodies (Fig. 2A), 225 mAb (at 0.5 and 2.0 μg/ml) and AG1478 (at 0.5 and 2.0 μM) effectively blocked EGF-induced EGFR tyrosine phosphorylation as detected by phosphotyrosine immunoblotting (Fig. 2C). The EGF-induced phosphorylation of MAPK, AKT and STAT3 was also completely inhibited by both 0.5 and 2.0 μM AG1478 (Fig. 2C). Significantly, 225 mAb at both 0.5 and 2.0 μg/ml only slightly inhibited the EGF-induced phosphorylation of these downstream signalling components (Fig. 2C), even though EGFR tyrosine phosphorylation was essentially completely inhibited. This demonstrates that in A549 cells there is a differential sensitivity of pathways downstream of EGFR to inhibition by AG1478 versus 225 mAb. This differential inhibition of downstream pathways conveniently provides us with an approach to determining, in the same cell system, which phosphorylated signalling molecules are most strongly associated with control of specific cell behaviors, such as growth and migration, i.e., we will be able to compare cell behavior under conditions in which EGFR phosphorylation is inhibited either with or without inhibition of MAPK, AKT and STAT3 phosphorylation.

Effect of EGFR modulation on monolayer growth. Although anchorage-dependent monolayer cell growth assays may be limited in their ability to predict in vivo responsiveness, they are conventionally used and form the basis for the NCI 60 tumor cell line panel in vitro screen for cytotoxic and cytostatic drugs.[50] We initiated our study of the behavior of A549 cells in various phenotypic assays by investigating the effects of EGF, 225 mAb and AG1478 on the monolayer growth of A549 cells using an established 3-[4,5-dimethylthiazol-2-yl]-2,5-diphenyltetrazolium bromide (MTT) metabolic dye-based read-out. As background, we examined the effect of EGF on monolayer growth in the presence and absence of various amounts of serum (Fig. 3A). These cells were able to grow in the absence of serum (doubling time of 45 hrs), with their proliferation being enhanced by increasing amounts of serum (up to 2-fold by 5% FBS; doubling time of approximately 24 hrs). In the absence of serum, EGF did not stimulate monolayer growth, even at 100 ng/ml. In media containing 5% serum, exogenous EGF slightly increased growth in a dose-dependent manner, i.e., 20% and 30% increases were observed in the presence of 10 and 100 ng/ml EGF, respectively. Both 225 mAb and AG1478 were able to inhibit the EGF-stimulated ~30% increase in monolayer growth that occurred in 5% serum (Fig. 3B), however they did not significantly inhibit basal monolayer growth in 5% serum. These results indicate that the monolayer growth of A549 cells is only modestly stimulated by exogenous EGF and that, in the absence of added EGF, it is not dependent on autocrine or serum-derived EGFR ligands. This provides an explanation for the relative insensitivity of conventional monolayer growth assays to detect the response of these cells to EGFR inhibitors.[29-33]

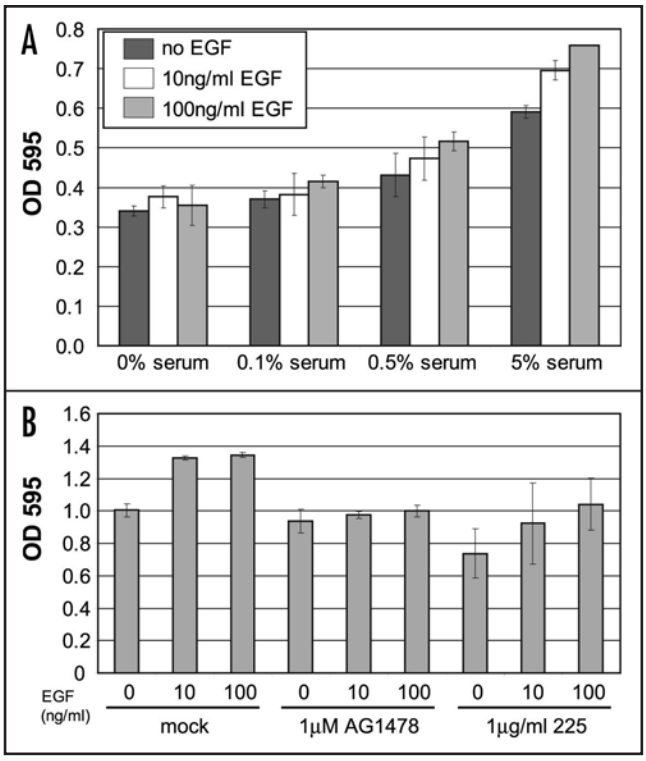

Figure 3. Effect of EGF and EGFR inhibitors on monolayer growth in A549 cells. Cells were plated at 2000 cells/well in a 96-well tissue culture plate with DMEM-5% FBS for 24 hours. (A) After serum starving for 2 hours, cells were incubated with various concentrations of serum and/ or EGF as indicated. (B) Cells were preincubated with 1 μM AG1478 or 1 μg/ml 225 mAb for 30 min prior to addition of EGF (0,10,100 ng/ml). After 72 hours, cell viability was assessed by adding MTT and measuring the absorbance at 595 nM (as described in Materials & Methods). Results shown are of a typical experiment performed in triplicate with associated standard deviations.

Effect of EGFR modulation on anchorage-independent growth. Despite the simplicity and convenience of short-term anchorage-dependent monolayer growth assays, they are limited in their ability to assess the potential clinical efficacy of compounds (see refs. 51-52). The soft agar clonogenic assay which measures colony formation by cells with the ability to grow under anchorage-independent conditions correlates better with cellular tumorigenicity in nude mice.[41] However, soft agar clonogenic assays are both labor-intensive and time-consuming (2–3 weeks incubation). In order to evaluate the effect of EGF and EGFR inhibitors on A549 cells in a more rapid and convenient test for anchorage-independent growth, we utilized a novel over-agar assay[53] in which cells are grown in suspension on top of a layer of agar for a 7-day period. This assay, which we adapted to measure viable cells by using a soluble metabolic dye (Alamar Blue), gives similar results to those obtained using a traditional soft agar growth assay (data not shown) but in a more expedient manner (see Materials and Methods).

To assess the effects of EGF and EGFR inhibitors on anchorage-independent proliferation/survival, we tested varying concentrations of AG1478 and 225 mAb on A549 cells plated under suspension conditions in the presence and absence of 50 ng/ml EGF (Fig. 4A). It can be seen that, in the absence of exogenous EGF, AG1478 and 225 mAb inhibited basal anchorage-independent growth in a

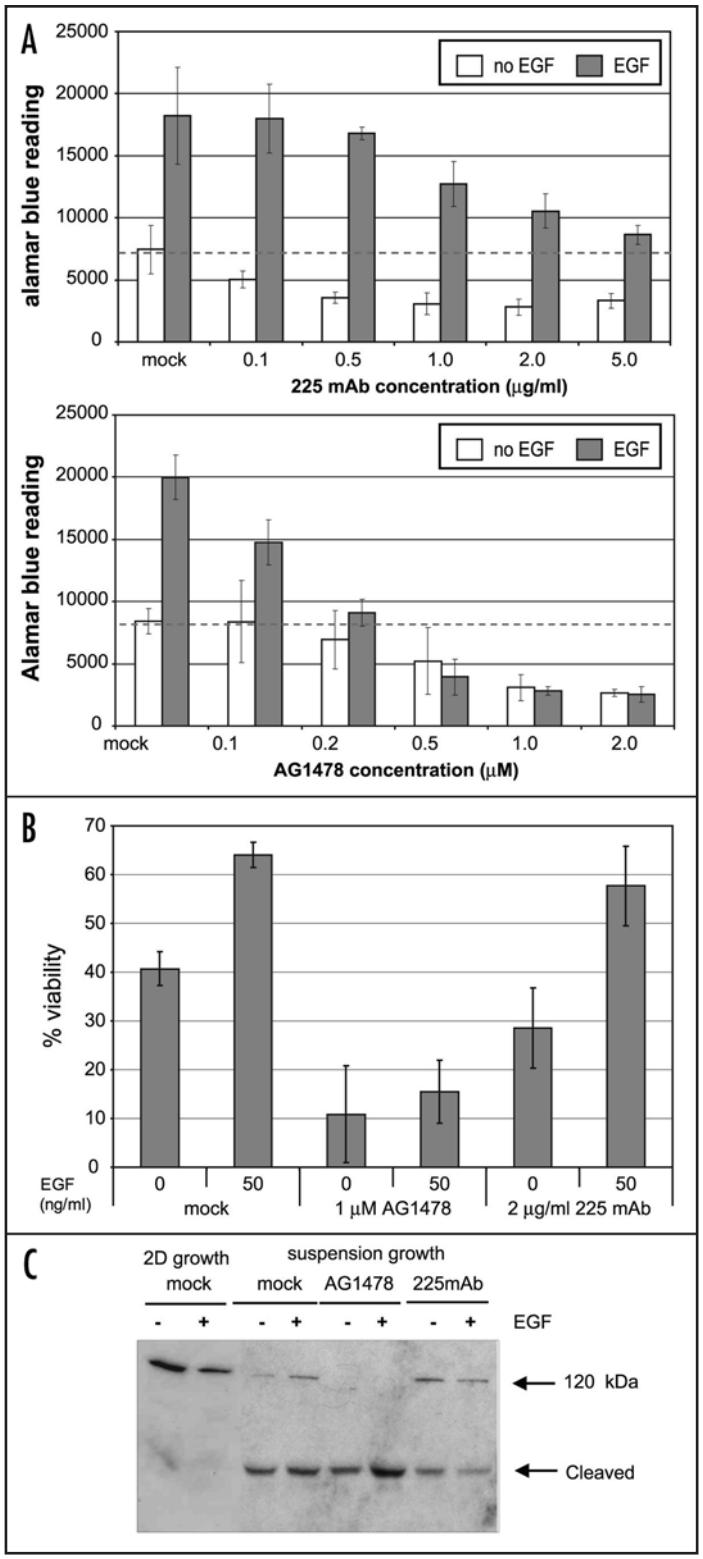

Figure 4. Effect of EGF and EGFR inhibitors on anchorage-independent growth and survival in A549 cells. Cells were plated on agarose-coated tissue culture plates to prevent adhesion and incubated for 7 days in various concentrations of EGF or EGFR inhibitors, 225 mAb or AG1478 (as indicated) prior to analysis of viable cell count using Alamar Blue as described in Materials and Methods. (A) Effect of increasing concentration of EGFR inhibitors on A549 anchorage-independent growth in the presence or absence of added EGF (50 ng/ml). (B) Cells were harvested after 7 day suspension growth and percent cell viability was assessed by live/dead staining with Calcein AM and propidium iodide followed by flow cytometry. Results shown are average of two experiments with associated s.e.m. (C) Analysis of full length and cleaved PARP was determined by Western blotting following 7-day incubation in monolayer or suspension cultures.

dose-dependent manner to a maximum of 60–70% (30–40% basal growth remaining, Fig. 4A). This demonstrates that, in contrast to monolayer growth, anchorage-independent basal growth of A549 cells is partially dependent on EGFR activity. Notably, the anchorage-independent growth of the A549 cells in the presence of 0.2 μM and higher concentrations of AG1478 was essentially the same in the presence and absence of added EGF. This suggests that these concentrations of AG1478 are able to block both EGF-stimulated and basal anchorage-independent growth relatively effectively. In contrast, at all concentrations of 225 mAb, anchorage-independent growth remained higher in the presence of exogenous EGF as compared to in its absence. This indicates that 225 mAb is relatively less potent in the presence of added EGF. This may reflect the competition between EGF and 225 mAb for binding to the extracellular domain of EGFR.

The effects of EGF and EGFR inhibitors on A549 cell anchorage-independent growth that we detected using the soluble metabolic dye, Alamar Blue, may result from changes in cell survival or division, or both. To determine the effects of EGFR modulation on cell viability under anchorage-independent conditions, we took advantage of the fact that, when using the over-agar assay, cells can be easily harvested. Accordingly, we were able to measure the percentage of viable cells by live/dead staining followed by flow cytometry (see Materials & Methods). The percentage of viable cells after 7 days of anchorage-independent growth was 41% (Fig. 4B) with the viability being increased to 64% by 50 ng/ml EGF, indicating that the stimulation of anchorage-independent growth by EGF reflects, at least partially, an increase in cell survival. AG1478 at 1 μM significantly decreased cell viability to a level of 11–15% both in the absence and presence of EGF, indicating that this inhibitor blocks basal and EGF-stimulated anchorage-independent growth due, at least in part, to its ability to reduce EGFR-dependent cell survival. 225 mAb at 2 μg/ml in the absence of EGF decreased the percentage of viable cells from 41% to 29%, but not to the extent induced by AG1478 (11–15%). In the presence of EGF, 225 mAb had no significant effect on cell survival. The fact that, in the presence of 50 ng/ml EGF, 225 mAb at 2 μg/ml significantly inhibited anchorage-independent growth (Fig. 4A) while having no effect on the percent of viable cells (Fig. 4B), implies that the effect of 225 mAb on anchorage-independent growth may be more reflective of its effect on cell division than on cell survival.

Since the differences in cell viability that we observed are likely related to anoikis, i.e., the apoptosis that occurs following loss of cell anchorage, we next examined the effects of EGF and EGFR inhibitors on apoptosis by monitoring the 85 kDa cleavage product of PARP, a caspase-3 substrate and a contributor to commitment to apoptosis.[54] The PARP cleavage product was detected in A549 cells grown under anchorage-independent conditions, but not under monolayer plating conditions (Fig. 4C), indicating that A549 cells indeed undergo anoikis when grown in an anchorage-independent environment. AG1478 enhanced PARP cleavage both in the absence and presence of EGF confirming that this inhibitor promotes anoikis and that it blocks basal and EGF-stimulated anchorage-independent

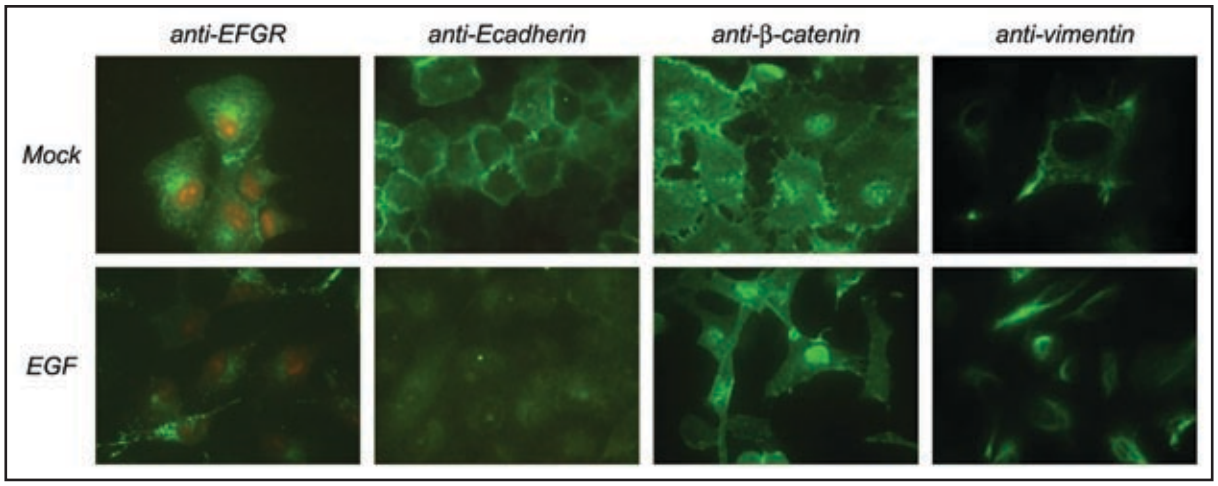

Figure 5. Effect of EGF on epithelial-to-mesenchymal transition in A549 cells. Indirect immunofluorescence analysis was performed with antibodies directed against EGFR and EMT markers (E-cadherin, β-catenin, vimentin) following incubation of A549 cells with 10 ng/ml EGF for 48 hrs as indicated in Materials and Methods.

growth due, in part, to its ability to reduce EGFR-dependent cell survival. Notably, 225 mAb failed to promote PARP cleavage in the absence or presence of EGF, indicating that 225 mAb does not significantly promote anoikis and that this underlies its lower ability to reduce cell viability under anchorage-independent conditions.

Effect of EGFR modulation on morphology and motility. During the course of these studies we noticed that EGF induced distinct morphological changes in A549 cells with characteristics similar to an epithelial-to-mesenchymal transition (EMT). EMT is a process by which epithelial cells lose epithelial features, including the presence of cell-adhesion molecules, and acquire migratory and/or invasive properties characteristic of mesenchymal cells. EMTs are necessary for morphogenetic movements of epithelial cells during development and are analogous to those that take place during the acquisition of an invasive phenotype in tumors of epithelial origin, reviewed in ref. 55.

EGF treatment promoted the dissociation of A549 cells that were clustered in a cobblestone fashion within epithelial "islands" and formation of spindle-shaped migratory fibroblast-like cells. Indirect immunofluorescence analysis was performed in order to determine if changes in the levels or subcellular localization of epithelial and mesenchymal markers, as well as EGFR, occur in A549 cells in response to EGF (Fig. 5). As expected, incubation with EGF for 48 hrs resulted in a dramatic internalization and downregulation of EGFR, as indicated by a sharp decrease in intensity of EGFR and a punctate intracellular staining profile reminiscent of late endosomes/lysosomes. E-cadherin, an epithelial cell adhesion molecule, was localized to the plasma membrane, particularly at sites of cell-cell contact, in untreated cells. Upon incubation, EGF induced a redistribution of E-cadherin resulting in a general diffuse intracellular staining pattern. In addition, beta-catenin, which is normally associated with E-cadherin on the inner leaflet of the plasma membrane in epithelial cells, was translocated predominantly to the nucleus in response to EGF. Vimentin, a mesenchymal marker, was expressed in untreated A549 cells, as has been demonstrated for a variety of epithelial cell lines cultured in vitro, however, its expression increased dramatically in the fibroblast shaped cells. Taken together these results are consistent with the morphological changes that are expected to occur upon an EMT-like transition.

Since cell motility changes generally correlate with EMT-like cell morphology changes and because EGFR overexpression has been implicated as promoting tumor cell motility and invasion in vitro[56,57] and in vivo,[58] we investigated the effects of EGF and EGFR inhibitors on cell motility using a scratch closure assay (Fig. 6A). In this assay, an area of confluent cells is removed using the end of a pipette tip and the rate of movement of cells into the denuded area is recorded. EGF stimulated motility, as evidenced by the filling of the area partially and fully, after 24 hr incubation with 10 ng/ml and 100 ng/ml EGF, respectively. EGF-stimulated motility was inhibited by AG1478 and 225 mAb, however, 225 mAb appeared to be less effective at blocking the motility induced by the higher concentration of EGF, once again illustrating the competitive nature of 225 mAb and EGF binding. In contrast, basal motility was not inhibited by 225 mAb and AG1478, indicating that the basal motility of these cells is not dependent on EGFR activity. These effects on motility were not due to changes in cell proliferation since EGF and EGFR inhibitors have a minor effect of monolayer cell growth (Fig. 3). In addition, mitomycin C, a drug that blocks the proliferation of these cells, failed to block EGF-induced motility (data not shown).

We also quantitatively analyzed motility using a recently established innovative method in which cells are plated at a low density on an ECM matrix in the presence of fluorescent beads.[44] Upon migration, the area is cleared thus leaving fluorescent-negative "tracks" on a fluorescent background, which can be quantitated using OpenLab software (see Materials and Methods). This clearing of a particle-free trail by a combination of cell locomotion and phagocytosis, described as "phagokinetics", has been used to quantify the motility of a variety of cell types.[59-61] In the fluorescent-negative track assay, EGF induced an approximate 2-fold increase in the area of the tracks formed on collagen (Fig. 6B, part 1 and 2). AG1478 and 225 mAb completely inhibited this EGF-stimulated motility, but did not inhibit basal motility in agreement with the scratch closure assay.

An advantage of this assay is that the intake of fluorescent beads into cells, which results from phagocytosis during locomotion, has been shown to correlate with motility in certain cell lines,[44]

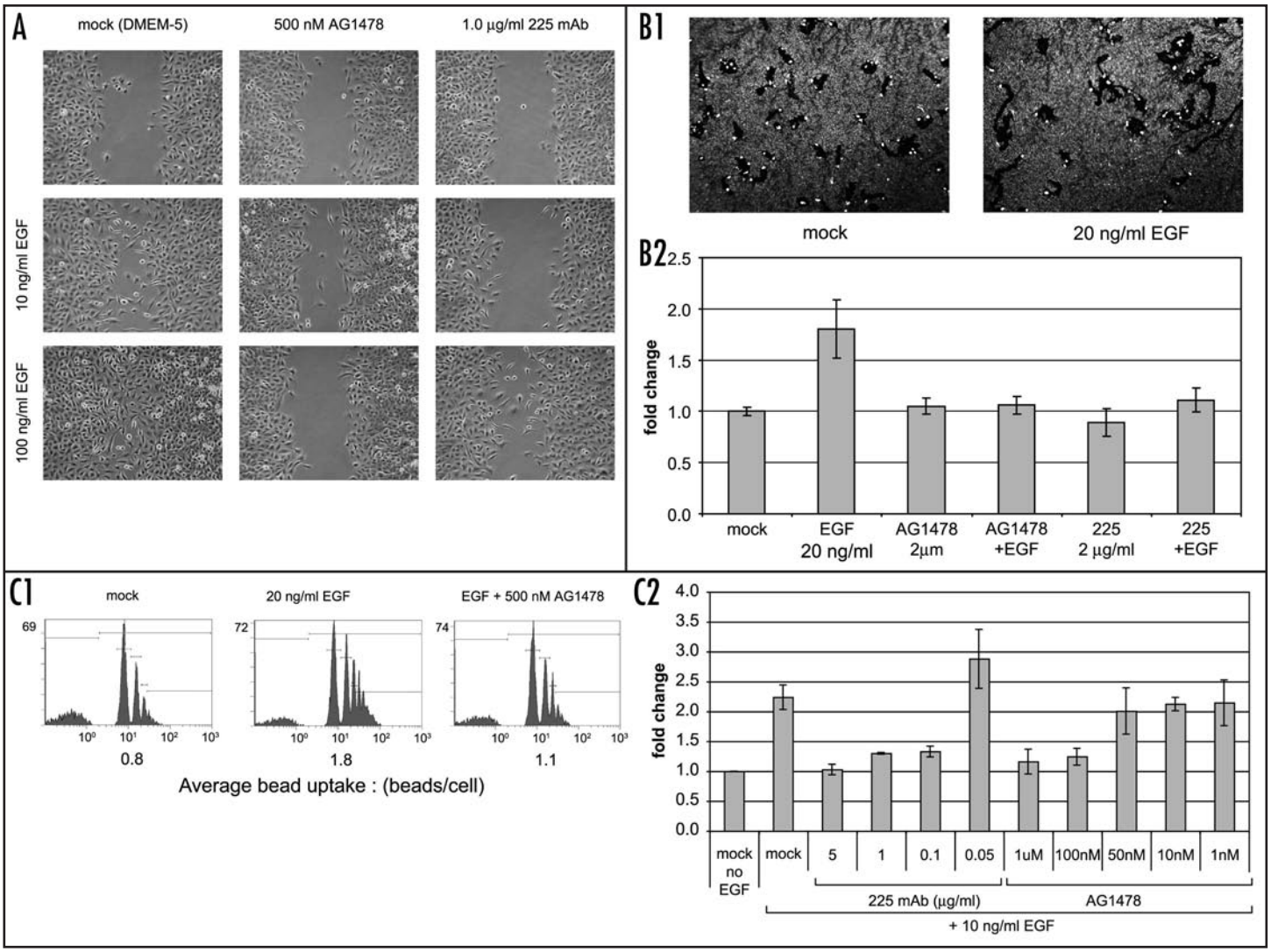

Figure 6. Effect of EGFR inhibitors on cell motility in A549. Various cell motility assays (as described in Materials and Methods) were used to measure the effects of EGF and/or EGFR inhibitors (as indicated). In the scratch closure assay, cell migration into the "scratched" denuded area is observed after 24 hrs incubation (A). In the track clearing assay, cells are plated on collagen in the presence of 0.025% fluorescent beads overnight and the area of the fluorescent-negative tracks which are created upon migration (B, part 1), are quantitated relative to the total number of cells in each field. Results shown are from a typical experiment in which the average of cleared area/cell from 4 independent fields of treated cells is analyzed relative to untreated cells (B, part 2). In the fluorescent phagokinetic assay, cells are plated on collagen in the presence of 0.001% fluorescent beads overnight and the intake of fluorescent beads into cells during the course of migration is analyzed by flow cytometry. Typical results of the distribution of the fluorescent beads in the A549 cell population is shown in the histogram with the average bead intake indicated (C, part 1). Quantitation of the phagokinetic assay relative to the average bead uptake of the untreated A549 cells (C, part 2). Results are shown in which the average bead uptake from of treated cells is analyzed relative to untreated cells (average of 3 experiments with associated standard deviation).

and can be sensitively quantified by flow cytometry. In Figure 6C, part 1, representative histograms are shown, which illustrate the distribution of fluorescent A549 cells following overnight incubation on plates coated with collagen and 0.001% fluorospheres. A heterogeneous population of cells can be detected by this method with varying levels of fluorescence. As can be seen, in the absence of EGF and AG1478, approximately 44% of cells were fluorescent, with an average bead uptake of 0.8 beads per cell. Upon incubation with 20 ng/ml EGF overnight, the proportion of cells that are fluorescent increases to 64% with an average bead uptake of 1.8 beads per cell, a 2.2 fold increase. The amount of EGF stimulation measured by bead uptake correlated well with the direct measurement of track clearing (i.e., 1.8 vs. 2.2 fold stimulation by EGF in the track clearing and bead uptake assay, respectively). AG1478 blocked the EGF-stimulated uptake of beads to a level similar to that in the absence of EGF (average bead uptake of 1.1 beads per cell). We further investigated the effect of EGF and the EGFR inhibitors on bead uptake by varying the concentration of 225 mAb and AG1478. Both 225 mAb and AG1478 completely inhibited EGF-stimulated bead uptake with as little as 100 ng/ml 225 mAb or 100 nM AG1478 , but had no effect on basal motility (Fig. 6C, part 2), which is consistent with the results obtained in the track clearing-based motility assay.

Discussion

The overall objective of this study was to examine the phenotypic

responses of A549 cells to EGF and EGFR inhibitors in a variety of in vitro assays and to correlate these responses with the phosphorylation of signalling pathway components. We chose to study the A549 NSCLC cell line in particular since this cell line model exhibits a discrepancy between its sensitivity to EGFR inhibitors in in vitro monolayer growth assays versus in animal xenograft models. Taking this into consideration, we were interested in comparing the efficacy of EGFR inhibitors in other clinically relevant biological assays related to tumor progression, namely anchorage-independent growth and motility assays. Also, by correlating these cell behaviors (monolayer growth, anchorage-independent growth, motility) with phosphorylation changes in signaling pathway components, we aimed to identify the pathway elements that were most strongly associated with different phenotypic behaviors. We utilized two EGFR inhibitors, the small molecule kinase inhibitor AG1478 and the ligand-blocking antibody 225 mAb, in order to compare the sensitivity of each assay to both inhibitors, and to have the potential for correlating differential effects of these two inhibitors on signaling pathways with disparities in phenotypic responses.

Our analysis of the effect of AG1478 and 225 mAb on signaling pathway phosphorylation events revealed that, at concentrations at which both 225 mAb and AG1478 were able to completely inhibit EGFR phosphorylation, only AG1478 was able to effectively inhibit EGF-induced MAPK, AKT and STAT3 phosphorylation (Fig. 2), demonstrating that these two inhibitors differentially affect signaling pathways downstream of EGFR. Since different inhibitor treatments may shift signal transduction kinetics in ways that are not noticeable from single time-point experiments, we further examined the effect of 225 mAb at additional time points after EGF stimulation. In agreement with our 10 minute time point, we observed a slight reduction in the magnitude of MAPK or Akt phosphorylation, with no obvious shift in the kinetics of phosphorylation in either A549 or HeLa cells (data not shown). The reason that 225 mAb is much less effective than AG1478 in the suppression of signals downsteam of EGFR is not clear. However, it could be that the differential effect of 225 mAb and AG1478 on internalization and trafficking of EGFR, which we have previously documented in A549 cells, may underlie this phenomenon. In our previous study, we demonstrated that 225 mAb, but not AG1478, induces EGFR internalization and weak downregulation in A549 cells via a mechanism distinct from that underlying EGF-induced EGFR internalization and downregulation.[28] Since certain signalling pathways are dependent upon internalization of EGFR for full activation,[48,62] differential internalization and routing of EGFR in response to 225 mAb versus AG1478 may impact on the effect of these inhibitors on downstream pathways, such as MAPK signalling. Although another explanation is that AG1478 may be acting non-specifically on kinases other than EGFR, which influence MAPK and PI3K signalling, this possibility seems unlikely at the concentrations of AG1478 used, i.e., ~1 μM. Another interesting finding in our signaling studies was the observation that 225 mAb, but not AG1478, varied in its ability to inhibit EGFR phosphorylation depending on the concentration of EGF. This is likely due to the fact that EGF competes with 225 mAb for binding to the extracellular domain of EGFR.

Our monolayer growth assays demonstrated that EGF had a modest stimulatory effect (25–30% increase) on growth (Fig. 3B) and that this increase was inhibited by both AG1478 and 225 mAb. The lack of inhibition of basal growth by AG14768 and 225 mAb indicates that these cells do not depend on an EGFR autocrine loop for basal monolayer growth and is consistent with other reports that evaluated the basal growth response of A549 cells in monolayer culture to other EGFR inhibitors such as gefitinib[30,31,33] and the chimeric version of 225 mAb, C225.[32]

In order to determine whether anchorage-independent growth of A549 cells was more sensitive than monolayer growth to EGF and EGFR inhibitors, we utilized a rapid and convenient over-agar assay. Our results demonstrating that both AG1478 and 225 mAb inhibit basal anchorage-independent growth indicates that, in contrast to monolayer growth, these cells rely at least in part on the presence of an EGFR ligand autocrine loop for anchorage-independent growth. We found that EGF stimulated anchorage-independent growth approximately 2-fold (Fig. 4A) and that AG1478 and 225 mAb reduced this stimulation, albeit to different extents. Although AG1478 was effective at inhibiting anchorage-independent growth in both in the presence and absence of EGF, 225 mAb was less effective in the presence of EGF (Fig. 4A). This likely occurs as a result of the competition between EGF and 225 mAb for binding to the extracellular domain of EGFR, and correlates with the effect of EGF on the ability of 225 mAb to block EGFR phosphorylation (Fig. 2A).

Extensive crosstalk exists between integrin and growth factor signalling pathways, including EGFR, which affects cell survival, differentiation and proliferation, reviewed in ref. 63. When cultured under anchorage-independent conditions in which integrin attachment is abrogated, cell anoikis, i.e., the apoptosis that occurs upon prevention of cell-matrix contact, is promoted. Because of this, effects on anchorage-independent growth may represent effects on both survival and cell division, rather than cell division alone.[64] Indeed, in this study, anchorage-independent conditions were found to enhance apoptosis as assessed by monitoring PARP cleavage (Fig. 4C). Additionally, the finding that EGF increased the percentage of viable cells indicates that EGF signaling promotes survival (Fig. 4B). Our studies on cell viability and apoptosis under anchorage-independent conditions also revealed that 225 mAb and AG1478 appear to differ with respect to the mechanism that they primarily use to affect anchorage-independent growth. Whereas AG1478 inhibited both basal and EGF-stimulated viability and promoted apoptosis (enhanced PARP cleavage), 225 mAb had limited effects on cell viability and no detectable effect on PARP cleavage (Fig. 4B and C). These observations suggest that 225 mAb inhibited anchorage-independent growth primarily by affecting events other than apoptosis, such as by inducing growth arrest, whereas AG1478 inhibited anchorage-independent growth primarily by reducing survival. The differential effect of 225 mAb and AG1478 on apoptosis/survival correlates with their differential effect on EGF-stimulated phosphorylation of MAPK, PI3K or STAT3 in A549 cells grown under monolayer (Fig. 2C) or anchorage-independent conditions (data not shown). This observation is in agreement with other studies demonstrating a role for PI3K and/or STAT3 as mediators of survival in NSCLC and other cell types.[14,17,65]

Our results demonstrating a strong inhibition of anchorage-independent growth and survival of A549 cells by AG1478 suggests that this type of EGFR inhibitor may block cell growth particularly well under circumstances in which cell survival is being reduced by therapeutic regimes such as chemotherapy or radiation. There is

evidence that other small molecule EGFR inhibitors synergize with radiation and/or chemotherapy to inhibit growth of NSCLC cell lines.[36-38,66] More specifically, in the study by Bianco et al (2002), a significant inhibition of A549 soft agar growth in vitro and tumor growth in mouse xenograft models was observed with the small molecule EGFR inhibitor ZD1839, which was enhanced by ionizing radiation.[37]

We also observed that EGF induced a striking loss of cell adhesion molecules (Fig. 5), and a concomitant scattering of A549 cells in a process resembling an EMT. Interestingly, we and others[67] have shown that untreated A549 cells express both mesenchymal markers, such as vimentin, as well as epithelial markers such as E-cadherin. These findings indicate that A549 cells may be prone to undergo an EMT-like process. The work of Thomson et al,[67] demonstrated that NSCLC cell lines that have undergone an EMT are more resistant to the growth inhibitory effects of the EGFR inhibitor, erlotinib. This leads to the idea that the tendency of A549 cells to express mesenchymal characteristics may underlie its low in vitro monolayer growth response to EGFR inhibitors. This premise is further supported by more recent findings in which a gene signature indicative of a mesenchymal phenotype is predictive of resistance to erlotinib-mediated growth inhibition in NSCLC cell lines.[68] Our current results indicate that A549 cells exhibit mesenchymal characteristics, particularly in the presence of EGF, and are relatively insensitive to EGFR inhibitors in monolayer growth assays, as expected. On the other hand, our results clearly demonstrate that A549 cells maintain the ability to respond sensitively to EGFR inhibitors in motility and survival assays.

As an additional phenotypic readout, we analyzed the effect of EGF and EGFR inhibitors on A549 cell motility using a variety of motility assays (Fig. 6). 225 mAb and AG1478 had no effect on the basal motility of A549 cells, indicating that their basal motility is not dependent on autocrine or serum-derived EGFR ligands. Using a novel quantitative flow cytometry-based assay, we observed that EGF stimulation resulted in a 2-fold increase in cell motility, and that this was completely inhibited by AG1478 (100 nM) and 225 mAb (100 ng/ml) (Fig. 6). Interestingly, the concentration of 225 mAb that inhibited EGF-stimulated motility was unable to inhibit EGF-induced MAPK, Akt or STAT3 signalling (Fig. 2C), suggesting that these molecules are not involved in EGF-stimulated motility in A549 cells. Other effectors such as PLCγ[69, 70] or FAK, which have been implicated in EGF-stimulated motility and invasion in A549[71] and other epithelial cell lines,[72] may be more tightly associated with motility. The dissection of which signalling molecules are most strongly associated with control of various cellular phenotypes is necessary for the derivation of models that are predictive of response to pathway inhibitors. At a systems biology level, Kumar et al,[73] recently identified, using mass spectrometry, elements of the signalling network of tyrosine phosphorylated proteins that govern HER2-mediated effects on migration and proliferation and derived predictive models accordingly.

In summary, the higher sensitivity of A549 cells to EGFR inhibitors in anchorage-independent cell growth and survival assays, as well as in cell motility assays, indicates that these assays are more predictive of the in vivo response of these cells. This may explain, in large part, the discrepancy between the sensitivity of A549 cell growth to EGFR inhibitors in in vitro conventional monolayer growth assays[29-33] versus in animal xenograft models.[34-38] Based on our results with A549 cells, we propose that EGF stimulates tumour progression of NSCLC primarily through effects on anchorage-independent growth/survival and motility and that assays measuring these cellular phenotypes are more appropriate for assessing EGFR inhibitor efficacy.

Materials and Methods

Antibodies and chemicals. Recombinant human EGF was purchased from AUSTRAL Biological. AG1478 was obtained from Calbiochem. Hybridoma expressing 225 antibody directed against the EGF receptor (ATCC HB-8508) was grown in DMEM/10% horse serum and 225 antibody purified using standard techniques Briefly, 50% ammonium sulfate precipitation was performed and the pellet dialyzed against and, resuspended in phosphate buffered saline (PBS) pH7.4. Affinity purification was then performed on donkey anti-mouse IgG column (Jackson ImmunoResearch), dialyzed against PBS and quantitated by BCA protein assay (Pierce). 225 mAb preparations were functionally tested for their ability to bind EGFR expressed on A549 cells by FACS analysis.

Antibodies used for Western blotting against EGFR (sc-03) HER2/neu (sc-284), erbB3 (sc-415) and ErbB-4 (sc-283) were obtained from Santa Cruz. Phospho-specific EGFR Y1068 was from Biosource International Inc. (Camarillo, CA). Other antibodies include monoclonal anti-β actin antibody (Sigma), anti-phosphotyrosine antibody (4G10, Upstate Biotechnology Incorporated), anti-PARP (Biomol SA250), anti-phosphoAkt Ser473 (Cell signalling # 9271) anti-phosphoMAPK pTEpY (Promega V8031) and anti-phosphoSTAT3 Y705 (Cell signalling # 9131).

Cell culture. Human Caucasian lung carcinoma cell (A549) were obtained from American Type Culture Collection and were grown in Dulbecco's modified Eagle's media (MultiCell, Wisent, Inc.) supplemented with 5% fetal bovine serum (Gibco) and 1% glutamine.

For detection of signalling pathways (EGFR, MAPK, Akt, STAT3), 100,000 cells were plated per well in a 12 well plate in 2 mls RPMI/5% FBS. The following day, the media was changed and replaced with EGFR inhibitors as indicated in RPMI/5% FBS and pre-incubated for 60 minutes prior to the addition of 200 µl EGF (supplied as a 10x concentrated stock, final concentration 10 or 100 ng/ml) for 10 minutes at 37°C. After aspiration of media, cells were lysed by the addition of boiling 2%SDS (100 ul/well).

Western blotting. Total cell lysates were prepared in boiling 2% SDS (50 ul/well in 24 well dish). 10 to 15 µl of lysate was loaded on a 7.5% polyacrylamide gel and analyzed by SDS gel electrophoresis. After transfer to nitrocellulose (Amersham), blots were blocked with 5% skim milk in TBS (10 mM Tris-CL pH7.5, 150 mM NaCl) containing 0.05% Tween-20. Blots were probed with antibodies (at their recommended dilutions) in 5% skim milk in TBS overnight at 4°C. Following detection with the appropriate horseradish-peroxidase conjugated secondary antibody (Jackson ImmunoResearch), blots were developed by enhanced chemiluminescence according to manufacturer's directions (Perkin Elmer Life Sciences). Quantitation of the Western blots was performed on an AlphaImager2200 using Alpha Imagev5.5 software (Alpha Innotech corp., San Leandro, CA).

Surface erbB detection by flow cytometry. Typically, A549 were cells plated at 250,000 cells per 100 mm dish the day before 72 hr treatment. Following incubation, cells were washed in PBS and

harvested by the addition of cell dissociation buffer (Sigma). Cells were suspended in PBS containing 10% FBS at 5 x 10^6 cells per ml and 200 µl were incubated with saturating amounts (2 µg or more) anti-EGFR (225 mAb) or erbB-2 (clone 9G6.10, Neomarkers, Labvision corporation, Fremont CA) antibodies for 2 h at 4°C. Following washes with PBS/FBS, cells were detected with saturating amounts of goat anti-mouse IgG Alexa 488 secondary antibodies (Molecular Probes). Alexa green fluorescence signal analyses were performed on viable cells gated on forward scattering, side scattering parameters and propidium iodide dye exclusion using a Coulter EPICS^{TM} XL-MCL flow Cytometer (Beckman-Coulter, Miami, Fl) and standard filter set. Since EGFR and erbB2 antibodies are of the same isotype (IgG1), their detection with secondary antibody should be comparable. Having previously calculated the amount of surface EGFR on these cells by Scatchard analysis, we compared the flow cytometry data (mean Intensity—background Intensity) for EGFR with that of erbB2 to estimate the cell surface erbB2 receptor density.

Growth and viability assays. For analyzing adherent cell growth, standard 3-[4,5-dimethylthiazol-2-yl]-2,5-diphenyltetrazolium bromide (MTT) assays were performed as previously described.[43] Briefly, A549 cells were plated at 2000 cells/well in a 96 well plated overnight in RPMI/5% FBS. Serum (FBS), EGF and EGFR inhibitors were added to their final concentrations (as indicated) in a final volume of 100 µl. After 48 hrs incubation at 37°C, 25 µl of MTT (2 mg/ml) was added and further incubated for 4 hrs at 37°C. The medium was then aspirated and the insoluble formazon product solubilized in 100 µl DMSO for 1 hr at 37°C. The absorbance at 595 nM was analyzed on a Molecular Devices Spectra Max 250 plate reader.

For analyzing suspension growth and viability, typically 500 µl of 1% agarose (Gibco) in RPMI was added to a 24 well dish and allowed to solidify. 50,000 A549 cells were plated in 500 µl RPMI containing 5% FBS. Inhibitors were added at 2X concentrations were indicated and cultures grown for 7 days at 37°C. 50 µl of Alamar Blue (Biosource) was added and incubated at 37°C for 2–4 hrs. The fluorescence of the reduced product was measured at an excitation wavelength of 530 nm and emission wavelength of 580 nm on a CytoFluor multiwell plate reader (PerSeptive Biosystems).

In some cases, live/dead staining of the resulting cell population was performed by incubating with calcein AM (4 µg/ml, Molecular Probes) and propidium iodide (10 µg/ml, Molecular Probes) prior to analysis by flow cytometry. Signal analyses were performed on cells gated on forward scattering, side scattering parameters using a Coulter EPICS^{TM} XL-MCL flow Cytometer (Beckman-Coulter, Miami, Fl) and standard filter set.

Indirect Immunofluorescence. A549 cells were grown on chamber slides to 50–80% confluency, exposed to 10 ng/ml EGF for 48 hrs at 37°C. Following incubation, cells were washed with PBS, fixed with 4% paraformaldehyde for 10 min, permeabilized with 0.1% Triton-X 100 for 10 min, and blocked with 4% serum for 1 h at room temperature. Cells were then incubated with anti-EGFR antibody (EGFR polyclonal sc-03, Santa Cruz Biotechnology; 1:50); anti-E-cadherin antibody (Zymed, 1:200); anti-beta-catenin antibody (Santa Cruz, 1:200); or anti-vimentin (ICN, 1:50) for 1 h at room temperature washed with PBS and then exposed to Alexa-488 labeled anti-mouse IgG or Alexa-568 labeled anti-rabbit IgG antibody (Molecular probes) for 1 hr at room temperature. The cells were then washed 3x times with PBS and mounted in fluorescent mounting medium (Antifade, Molecular Probes). As negative controls, primary antibodies were omitted and secondary antibodies were used alone. Fluorescent images were captured using a Coolsnap CCD digital camera mounted on a Leitz upright microscope.

Motility based assays. Assays were performed essentially as previously described[44] with some minor modifications . For track clearing assays, plates were coated with 50 µg/ml collagen in 0.1 N acetic acid (Sigma #C7661) for one hour to overnight at 4°C and washed with PBS, before coating with 0.025% (v/v) Fluospheres (Molecular Probes #F-8823) in PBS for four hours to overnight at 4°C. Plates were washed 3 times with PBS to remove unattached beads, and cells were plated at low density (12 cells/mm^2). Once attached, cells were treated with inhibitors 30 minutes prior to addition of EGF. After 20 hours incubation, cells were fixed with 3% paraformaldehyde (PBS) and fluorescent images were photographed at low magnification using a Qimaging Retiga 2000R Fast1394 digital camera mounted on a Leica DMIL upright microscope. Track clearing quantification was performed after binary mask analysis of at least four fields per view, minimum 200 cells analyzed (Openlab software, Improvision).

For flow cytometry analysis of motility, cells plated on collagen plates which were coated with a lower density of fluorescent beads (0.001% (v/v) Fluospheres) and treated as above for track clearing. Cells were collected after 20 hours by trypsinization, and analyzed by flow cytometry. Green fluorescence signal analyses were performed on viable cells gated on forward scattering, side scattering parameters using a Coulter EPICS^{TM} XL-MCL flow Cytometer (Beckman-Coulter, Miami, Fl) and standard filter set.

Acknowledgements

We are grateful to Anjenn Chenn for helpful advice regarding the fluorescent bead based motility assay, to Antoine Caron for excellent technical assistance with imaging analysis as well as to Andre Migneault for the preparation of figures. This article is National Research Council (NRC) Publication No. 49520.

References

1. Jemal A, Clegg LX, Ward E, Ries LA, Wu X, Jamison PM, Wingo PA, Howe HL, Anderson RN, Edwards BK. Annual report to the nation on the status of cancer, 1975-2001, with a special feature regarding survival. Cancer 2004; 101:3-27.
2. Hirsch FR, Varella Garcia M, Bunn PA, Jr., Di Maria MV, Veve R, Bremmes RM, Baron AE, Zeng C, Franklin WA. Epidermal growth factor receptor in non-small-cell lung carcinomas: correlation between gene copy number and protein expression and impact on prognosis. J Clin Oncol 2003; 21:3798-807.
3. Salomon DS, Brandt R, Ciardiello F, Normanno N. Epidermal growth factor-related peptides and their receptors in human malignancies. Critical reviews in oncology/hematology 1995; 19:183-232.
4. Hynes NE, Lane HA. ERBB receptors and cancer: the complexity of targeted inhibitors. Nat Rev Cancer 2005; 5:341-54.
5. Levitzki A, Mishani E. Tyrphostins and other tyrosine kinase inhibitors. Annual review of biochemistry 2006; 75:93-109.
6. Ellis AG, Doherty MM, Walker F, Weinstock J, Nerrie M, Vitali A, Murphy R, Johns TG, Scott AM, Levitzki A, McLachlan G, Webster LK, Burgess AW, Nice EC. Preclinical analysis of the analinoquinazoline AG1478, a specific small molecule inhibitor of EGF receptor tyrosine kinase. Biochemical pharmacology 2006; 71:1422-34.
7. Cohen MH, Williams GA, Sridhara R, Chen G, Pazdur R. FDA drug approval summary: gefitinib (ZD1839) (Iressa) tablets. The oncologist 2003; 8:303-6.
8. Cohen MH, Johnson JR, Chen YF, Sridhara R, Pazdur R. FDA drug approval summary: erlotinib (Tarceva) tablets. The oncologist 2005; 10:461-6.
9. Harding J, Burtness B. Cetuximab: an epidermal growth factor receptor chemeric human-murine monoclonal antibody. Drugs Today (Barc) 2005; 41:107-27.
10. Humblet Y. Cetuximab: an IgG(1) monoclonal antibody for the treatment of epidermal growth factor receptor-expressing tumours. Expert opinion on pharmacotherapy 2004; 5:1621-33.
11. Labianca R, La Verde N, Garassino MC. Development and clinical indications of cetuximab. The International journal of biological markers 2007; 22:S40-6.

12. Marmor MD, Skaria KB, Yarden Y. Signal transduction and oncogenesis by ErbB/HER receptors. International journal of radiation oncology, biology, physics 2004; 58:903-13.
13. Huang C, Jacobson K, Schaller MD. MAP kinases and cell migration. Journal of cell science 2004; 117:4619-28.
14. Brader S, Eccles SA. Phosphoinositide 3-kinase signalling pathways in tumor progression, invasion and angiogenesis. Tumori 2004; 90:2-8.
15. Jing N, Tweardy DJ. Targeting Stat3 in cancer therapy. Anti-cancer drugs 2005; 16:601-7.
16. Gao SP, Bromberg JF. Touched and moved by STAT3. Sci STKE 2006; 2006:30.
17. Haura EB, Zheng Z, Song L, Cantor A, Bepler G. Activated epidermal growth factor receptor-Stat-3 signaling promotes tumor survival in vivo in non-small cell lung cancer. Clin Cancer Res 2005; 11:8288-94.
18. Mitsudomi T, Viallet J, Mulshine JL, Linnoila RI, Minna JD, Gazdar AF. Mutations of ras genes distinguish a subset of non-small-cell lung cancer cell lines from small-cell lung cancer cell lines. Oncogene 1991; 6:1353-62.
19. Monks A, Scudiero D, Skehan P, Shoemaker R, Paull K, Vistica D, Hose C, Langley J, Cronise P, Vaigro-Wolff A, et al. Feasibility of a high-flux anticancer drug screen using a diverse panel of cultured human tumor cell lines. Journal of the National Cancer Institute 1991; 83:757-66.
20. Mase K, Iijima T, Nakamura N, Takeuchi T, Onizuka M, Mitsui T, Noguchi M. Intrabronchial orthotopic propagation of human lung adenocarcinoma—characterizations of tumorigenicity, invasion and metastasis. Lung Cancer 2002; 36:271-6.
21. Onn A, Isobe T, Itasaka S, Wu W, O'Reilly MS, Ki Hong W, Fidler IJ, Herbst RS. Development of an orthotopic model to study the biology and therapy of primary human lung cancer in nude mice. Clin Cancer Res 2003; 9:5532-9.
22. Kraus Berthier L, Jan M, Guilbaud N, Naze M, Pierre A, Atassi G. Histology and sensitivity to anticancer drugs of two human non-small cell lung carcinomas implanted in the pleural cavity of nude mice. Clin Cancer Res 2000; 6:297-304.
23. Nogawa M, Yuasa T, Kimura S, Kuroda J, Sato K, Segawa H, Yokota A, Maekawa T. Monitoring luciferase-labeled cancer cell growth and metastasis in different in vivo models. Cancer letters 2005; 217:243-53.
24. Kang Y, Omura M, Suzuki A, Oka T, Nakagami Y, Cheng C, Nagashima Y, Inoue T. Development of an orthotopic transplantation model in nude mice that simulates the clinical features of human lung cancer. Cancer science 2006; 97:996-1001.
25. Paez JG, Janne PA, Lee JC, Tracy S, Greulich H, Gabriel S, Herman P, Kaye FJ, Lindeman N, Boggon TJ, Naoki K, Sasaki H, Fujii Y, Eck MJ, Sellers WR, Johnson BE, Meyerson M. EGFR mutations in lung cancer: correlation with clinical response to gefitinib therapy. Science 2004; 304:1497-500.
26. Lynch TJ, Bell DW, Sordella R, Gurubhagavatula S, Okimoto RA, Brannigan BW, Harris PL, Haserlat SM, Supko JG, Haluska FG, Louis DN, Christiani DC, Settleman J, Haber DA. Activating mutations in the epidermal growth factor receptor underlying responsiveness of non-small-cell lung cancer to gefitinib. The New England journal of medicine 2004; 350:2129-39.
27. Pao W, Miller VA. Epidermal growth factor receptor mutations, small-molecule kinase inhibitors, and non-small-cell lung cancer: current knowledge and future directions. J Clin Oncol 2005; 23:2556-68.
28. Jaramillo ML, Leon Z, Grothe S, Paul-Roc B, Abulrob A, O'Connor McCourt M. Effect of the anti-receptor ligand-blocking 225 monoclonal antibody on EGF receptor endocytosis and sorting. Experimental cell research 2006; 312:2778-90.
29. Bishop PC, Myers T, Robey R, Fry DW, Liu ET, Blagosklonny MV, Bates SE. Differential sensitivity of cancer cells to inhibitors of the epidermal growth factor receptor family. Oncogene 2002; 21:119-27.
30. Ono M, Hirata A, Kometani T, Miyagawa M, Ueda S, Kinoshita H, Fujii T, Kuwano M. Sensitivity to gefitinib (Iressa, ZD1839) in non-small cell lung cancer cell lines correlates with dependence on the epidermal growth factor (EGF) receptor/extracellular signal-regulated kinase 1/2 and EGF receptor/Akt pathway for proliferation. Molecular cancer therapeutics 2004; 3:465-72.
31. Nakamura H, Takamori S, Fujii T, Ono M, Yamana H, Kuwano M, Shirouzu K. Cooperative cell-growth inhibition by combination treatment with ZD1839 (Iressa) and trastuzumab (Herceptin) in non-small-cell lung cancer. Cancer letters 2005; 230:33-46.
32. Janmaat ML, Kruyt FA, Rodriguez JA, Giaccone G. Response to epidermal growth factor receptor inhibitors in non-small cell lung cancer cells: limited antiproliferative effects and absence of apoptosis associated with persistent activity of extracellular signal-regulated kinase or Akt kinase pathways. Clin Cancer Res 2003; 9:2316-26.
33. Noro R, Gemma A, Kosaihira S, Kokubo Y, Chen M, Seike M, Kataoka K, Matsuda K, Okano T, Minegishi Y, Yoshimura A, Kudoh S. Gefitinib (IRESSA) sensitive lung cancer cell lines show phosphorylation of Akt without ligand stimulation. BMC cancer 2006; 6:277.
34. Morelli MP, Cascone T, Troiani T, Tuccillo C, Bianco R, Normanno N, Romano M, Veneziani BM, Fontanini G, Eckhardt SG, De Pacido S, Tortora G, Ciardiello F. Antitumor activity of the combination of cetuximab, an anti-EGFR blocking monoclonal antibody and ZD6474, an inhibitor of VEGFR and EGFR tyrosine kinases. Journal of cellular physiology 2006; 208:344-53.
35. Steiner P, Joynes C, Bassi R, Wang S, Tonra JR, Hadari YR, Hicklin DJ. Tumor growth inhibition with cetuximab and chemotherapy in non-small cell lung cancer xenografts expressing wild-type and mutated epidermal growth factor receptor. Clin Cancer Res 2007; 13:1540-51.
36. Raben D, Helfrich BA, Chan D, Johnson G, Bunn PA, Jr. ZD1839, a selective epidermal growth factor receptor tyrosine kinase inhibitor, alone and in combination with radiation and chemotherapy as a new therapeutic strategy in non-small cell lung cancer. Seminars in oncology 2002; 29:37-46.
37. Bianco C, Tortora G, Bianco R, Caputo R, Veneziani BM, Caputo R, Damiano V, Troiani T, Fontanini G, Raben D, Pepe S, Bianco AR, Ciardiello F. Enhancement of antitumor activity of ionizing radiation by combined treatment with the selective epidermal growth factor receptor-tyrosine kinase inhibitor ZD1839 (Iressa). Clin Cancer Res 2002; 8:3250-8.
38. Higgins B, Kolinsky K, Smith M, Beck G, Rashed M, Adames V, Linn M, Wheeldon E, Gand L, Birnboeck H, Hoffmann G. Antitumor activity of erlotinib (OSI-774, Tarceva) alone or in combination in human non-small cell lung cancer tumor xenograft models. Anti-cancer drugs 2004; 15:503-12.
39. Ellis LM. Epidermal growth factor receptor in tumor angiogenesis. Hematology/oncology clinics of North America 2004; 18:1007-21.
40. Walker JL, Fournier AK, Assoian RK. Regulation of growth factor signaling and cell cycle progression by cell adhesion and adhesion-dependent changes in cellular tension. Cytokine & growth factor reviews 2005; 16:395-405.
41. Shin SI, Freedman VH, Risser R, Pollack R. Tumorigenicity of virus-transformed cells in nude mice is correlated specifically with anchorage independent growth in vitro. Proceedings of the National Academy of Sciences of the United States of America 1975; 72:4435-9.
42. Norton L, Massague J. Is cancer a disease of self-seeding? Nature medicine 2006; 12:875-8.
43. Mosmann T. Rapid colorimetric assay for cellular growth and survival: application to proliferation and cytotoxicity assays. Journal of immunological methods 1983; 65:55-63.
44. Windler Hart SL, Chen KY, Chenn A. A cell behavior screen: identification, sorting, and enrichment of cells based on motility. BMC cell biology [electronic resource] 2005; 6:14.
45. Rachwal WJ, Bongiorno PF, Orringer MB, Whyte RI, Ethier SP, Beer DG. Expression and activation of erbB-2 and epidermal growth factor receptor in lung adenocarcinomas. British journal of cancer 1995; 72:56-64.
46. Gollamudi M, Nethery D, Liu J, Kern JA. Autocrine activation of ErbB2/ErbB3 receptor complex by NRG-1 in non-small cell lung cancer cell lines. Lung Cancer 2004; 43:135-43.
47. Jorissen RN, Walker F, Pouliot N, Garrett TP, Ward CW, Burgess AW. Epidermal growth factor receptor: mechanisms of activation and signalling. Experimental cell research 2003; 284:31-53.
48. Yarden Y, Sliwkowski MX. Untangling the ErbB signalling network. Nature reviews 2001; 2:127-37.
49. Gill GN, Kawamoto T, Cochet C, Le A, Sato JD, Masui H, McLeod C, Mendelsohn J. Monoclonal anti-epidermal growth factor receptor antibodies which are inhibitors of epidermal growth factor binding and antagonists of epidermal growth factor binding and antagonists of epidermal growth factor-stimulated tyrosine protein kinase activity. The Journal of biological chemistry 1984; 259:7755-60.
50. Shoemaker RH. The NCI60 human tumour cell line anticancer drug screen. Nat Rev Cancer 2006; 6:813-23.
51. Brown JM. NCI's anticancer drug screening program may not be selecting for clinically active compounds. Oncology research 1997; 9:213-5.
52. Zips D, Thames HD, Baumann M. New anticancer agents: in vitro and in vivo evaluation. In vivo (Athens, Greece) 2005; 19:1-7.
53. Dong Z, Cmarik JL. Harvesting cells under anchorage-independent cell transformation conditions for biochemical analyses. Sci STKE 2002; 2002:7.
54. Trucco C, Oliver FJ, de Murcia G, Menissier de Murcia J. DNA repair defect in poly(ADP-ribose) polymerase-deficient cell lines. Nucleic acids research 1998; 26:2644-9.
55. Hay ED. An overview of epithelio-mesenchymal transformation. Acta anatomica 1995; 154:8-20.
56. Wells A. Tumor invasion: role of growth factor-induced cell motility. Advances in cancer research 2000; 78:31-101.
57. Yang Z, Bagheri Yarmand R, Wang RA, Adam L, Papadimitrakopoulou VV, Clayman GL, El Naggar A, Lotan R, Barnes CJ, Hong WK, Kumar R. The epidermal growth factor receptor tyrosine kinase inhibitor ZD1839 (Iressa) suppresses c-Src and Pak1 pathways and invasiveness of human cancer cells. Clin Cancer Res 2004; 10:658-67.
58. Xue C, Wyckoff J, Liang F, Sidani M, Violini S, Tsai KL, Zhang ZY, Sahai E, Condeelis J, Segall JE. Epidermal growth factor receptor overexpression results in increased tumor cell motility in vivo coordinately with enhanced intravasation and metastasis. Cancer research 2006; 66:192-7.
59. al Moustafa AE, Urbani N, O'Connor-McCourt M. Black cellular spreading and motility assay. BioTechniques 1999; 27:60-2.
60. Albrecht Buehler G. The phagokinetic tracks of 3T3 cells. Cell 1977; 11:395-404.
61. Scott WN, McCool K, Nelson J. Improved method for the production of gold colloid monolayers for use in the phagokinetic track assay for cell motility. Analytical biochemistry 2000; 287:343-4.
62. Clague MJ, Urbe S. The interface of receptor trafficking and signalling. Journal of cell science 2001; 114:3075-81.
63. Danen EH. Integrins: regulators of tissue function and cancer progression. Current pharmaceutical design 2005; 11:881-91.
64. Reddig PJ, Juliano RL. Clinging to life: cell to matrix adhesion and cell survival. Cancer metastasis reviews 2005; 24:425-39.
65. Song L, Turkson J, Karras JG, Jove R, Haura EB. Activation of Stat3 by receptor tyrosine kinases and cytokines regulates survival in human non-small cell carcinoma cells. Oncogene 2003; 22:4150-65.
66. Tortora G, Gelardi T, Ciardiello F, Bianco R. The rationale for the combination of selective EGFR inhibitors with cytotoxic drugs and radiotherapy. The International journal of biological markers 2007; 22:47-52.

67. Thomson S, Buck E, Petti F, Griffin G, Brown E, Ramnarine N, Iwata KK, Gibson N, Haley JD. Epithelial to mesenchymal transition is a determinant of sensitivity of non-small-cell lung carcinoma cell lines and xenografts to epidermal growth factor receptor inhibition. Cancer research 2005; 65:9455-62.
68. Yauch RL, Januario T, Eberhard DA, Cavet G, Zhu W, Fu L, Pham TQ, Soriano R, Stinson J, Seshagiri S, Modrusan Z, Lin CY, O'Neill V, Amler LC. Epithelial versus mesenchymal phenotype determines in vitro sensitivity and predicts clinical activity of erlotinib in lung cancer patients. Clin Cancer Res 2005; 11:8686-98.
69. Wells A, Kassis J, Solava J, Turner T, Lauffenburger DA. Growth factor-induced cell motility in tumor invasion. Acta oncologica (Stockholm, Sweden) 2002; 41:124-30.
70. Wells A, Ware MF, Allen FD, Lauffenburger DA. Shaping up for shipping out: PLCgamma signaling of morphology changes in EGF-stimulated fibroblast migration. Cell motility and the cytoskeleton 1999; 44:227-33.
71. Hauck CR, Sieg DJ, Hsia DA, Loftus JC, Gaarde WA, Monia BP, Schlaepfer DD. Inhibition of focal adhesion kinase expression or activity disrupts epidermal growth factor-stimulated signaling promoting the migration of invasive human carcinoma cells. Cancer research 2001; 61:7079-90.
72. Lu Z, Jiang G, Blume-Jensen P, Hunter T. Epidermal growth factor-induced tumor cell invasion and metastasis initiated by dephosphorylation and downregulation of focal adhesion kinase. Molecular and cellular biology 2001; 21:4016-31.
73. Kumar N, Wolf Yadlin A, White FM, Lauffenburger DA. Modeling HER2 effects on cell behavior from mass spectrometry phosphotyrosine data. PLoS computational biology 2007; 3:4.